

LASER TECHNOLOGIES

PACS numbers: 42.55.Lt; 42.55.Wd; 42.62.Cf
DOI: 10.1070/QE2015v045n09ABEH015739

Experimental comparison of laser energy losses in high-quality laser-oxygen cutting of low-carbon steel using radiation from fibre and CO_2 lasers

A.A. Golyshev, A.G. Malikov, A.M. Orishich, V.B. Shulyat'ev

Abstract. **We report a comparative experimental study of laser-oxygen cutting of low-carbon steel using a fibre laser with a wavelength of 1.07 μm and a CO_2 laser with a wavelength of 10.6 μm at the sheet thickness of 3–16 mm. For the two lasers we have measured the dependence of the cutting speed on the radiation power and determined the cutting speed at which the surface roughness is minimal. The coefficient of laser radiation absorption in the laser cutting process is measured for these lasers at different values of the cutting speed and radiation power. It is found that the minimal roughness of the cut surface is reached at the absorbed laser energy per unit volume of the removed material, equal to 11–13 J mm^{-3}; this value is the same for the two lasers and does not depend on the sheet thickness.**

Keywords: *laser-oxygen cutting, fibre laser, CO_2 laser, cut quality, optimisation, absorption coefficient, specific energy absorption.*

1. Introduction

During the last decade, laser cutting of metals by means of radiation from solid-state fibre and disk lasers with a wavelength of about 1 μm has been actively studied and applied. The first experimental results showed that the characteristics of cutting, namely, speed, cut surface quality and its dependence on the thickness of the cut sheet, are different for solid-state and CO_2 lasers. Fibre lasers allow one to obtain a high cutting speed and high cut quality in the case of thin sheets (up to 3–4 mm) [1]. If the sheet thickness is large, the speed difference decreases and becomes negligible, while the cut surface roughness (characteristic value of ripples, which in most cases is taken as the main indicator of cut quality) in the case of a fibre laser is greater than that for a CO_2 laser.

In studies on laser cutting, fundamental physical mechanisms are being sought for to explain the difference in characteristics of cutting, proceeding from the radiation parameters [2–4]. The coefficient of radiation absorption for metals differently depends on the angle of incidence at wavelengths of 1.07 and 10.6 μm. At normal incidence, the absorption coefficient is greater for radiation from a fibre laser, while at small angles between the beam axis and surface – for radiation from a CO_2 laser [5]. Spatial characteristics of the two lasers are also different, which results in different shape of the cut channel and different absorption on channel walls [5, 6].

Hirano and Fabbro [7] have analysed the wavefront stability with respect to small variations in the radiation intensity of fibre and CO_2 lasers. According to [7], with the absorption coefficient dependence on the angle of incidence being characteristic of each laser, local variations in the cut front profiles produce changes in the absorption coefficient, which contribute to an increase in arising inhomogeneities in the case of a fibre laser and their decrease in the case of a CO_2 laser. It has been assumed that this may be a cause of instability of the cut front and increased roughness of the cut surface in the case of a fibre laser. In the experiments on cutting cold-work tool steel by disk and CO_2 lasers, Scintilla et al. [8] found that the surface of the cut front may be irregular and have areas with a negative slope. In the case of a disk laser, a greater slope and edge ripples are observed. The authors attribute this to the possibility of multiple reflection of radiation from the walls of the cut channel, which is more pronounced for radiation with a wavelength of 1 μm. Petring et al. [4] performed a numerical simulation of laser cutting and drew a conclusion as to the necessity of accounting for multiple reflections in the energy balance of cutting and shaping the cut front. At a laser wavelength of 1 μm, multiple reflections may lead to formation of 'hot spots' inside the cut channel, i.e., the areas with an increased energy release, which may also be a cause of surface defects and deterioration of the cut quality.

In [3, 8], the coefficient of laser radiation absorption is measured and a comparison of the energy balance in cutting tool steel using disk and CO_2 lasers with inert gas is performed. According to the study, the melt has a lower temperature in the case of a disk laser. Scintilla et al. [8] use this fact to explain a larger volume of a remelted metal layer remaining on the cut walls and the worst quality of the cut surface compared to the case of a CO_2 laser, because at a lower temperature, the melt has a higher viscosity, and the effectiveness of its removal from the cut channel is less. However, in the calculations [4], the cut front temperature obtained for the case of cutting with the use of a fibre laser is higher compared to that for the case of a CO_2 laser. The authors of [4] consider the increased absorption of radiation on the walls, which occurs in the course of multiple reflections, to be a possible cause for a larger volume of remelted metal.

Thus, to date there is no full clarity as to the reasons why different radiation characteristics of fibre and CO_2 lasers lead to different characteristics of the relevant cut. The proposed explanations do not have a reliable physical basis, which, among other reasons, is related to the lack of experimental

A.A. Golyshev, A.G. Malikov, A.M. Orishich, V.B. Shulyat'ev
S.A. Khristianovich Institute of Theoretical and Applied Mechanics, Siberian Branch, Russian Academy of Sciences, Institutskaya ul. 4/1, 630090 Novosibirsk, Russia; e-mail: elexgol@cn.ru, smalik@ngs.ru, orishich@itam.nsc.ru, laser@itam.nsc.ru

Received 24 December 2014; revision received 1 April 2015
Kvantovaya Elektronika **45** (9) 873–878 (2015)
Translated by M.A. Monastyrskiy

data on comparative studies of cutting using two types of lasers under comparable conditions. This is especially true for laser-oxygen cutting. In a recent study, Pocorni et al. [9] made an experimental comparison of the separation energy (the laser energy required to create a unit surface of the laser cut) for laser-oxygen cutting by means of fibre and CO_2 lasers. However, the separation energy was calculated relative to the incident power, and the measurements of the coefficient of laser radiation absorption and energy balance were not carried out. In the present work, we measured, for the first time, the coefficient of laser radiation absorption and presented a detailed experimental comparison of the losses of absorbed laser energy in high-quality laser-oxygen cutting of low-carbon steel using fibre and CO_2 lasers.

2. Experimental technique

A 2-kW IPG/IRE-Polus ytterbium laser with an IPG collimator (D5-WC/AC model) is used for cutting. The beam parameter product (BPP), i.e., the product of the beam radius in the near field by the beam angular radius in the far field, is equal to 3.8 mm mrad. The beam diameter on the focusing lens after passing the collimator amounts to 17 mm; the lens focal length is 200 mm. The radiation power is varied in the range from 0.5 to 2 kW. A continuous CO_2 laser with a BPP equal to 4.7 mm mrad is also used [10]. Cutting is carried out according to traditional scheme by means of circularly polarised radiation at a radiation power of 0.5 to 3.5 kW. The radiation is focused by a ZnSe lens with a focal length of 190.5 mm. The beam diameter on the lens is 25 mm. The fibre laser is used to cut the sheets of 3-, 5- and 10-mm-thick St3ps low-carbon steel, while the CO_2 laser is used for cutting the sheets of 5, 10 and 16 mm in thickness. The oxygen jet is formed by a conical nozzle at a gage pressure of 0.25 MPa in a gas chamber of the laser cutter when cutting 3-mm-thick sheets and 0.05 MPa for all other thicknesses.

The value of surface roughness of the cut (typical height of ripples) is measured using an Olympus LEXT laser scanning confocal microscope near the upper and lower surfaces of the sheet. A larger value of the two measurements is taken as the sample characteristic. The techniques of determining the optimal values of the cutting speed and the cut width are based on measuring the dependence of cutting parameters on roughness and described in detail in [11, 12].

The absorption coefficient A is measured during cutting by the method described in [13, 14] and determined from the relation

$$A = \frac{W - W_{\text{tr}}}{W},$$

where W_{tr} is the power of radiation passed through the laser cut. The measurement process is shown schematically in Fig. 1.

The power meter is mounted on a tripod being mechanically connected with a laser cutter and moving with it during the cutting process. We have used an OPHIR 5000W-CAL-SH power meter. A flow of metal particles and oxides from the cut channel is blown away by the lateral air jet and does not hit the receiving area of the power meter.

3. Experimental results

In the preliminary series of experiments, the focusing lens and the oxygen pressure in the laser cutter chamber were selected

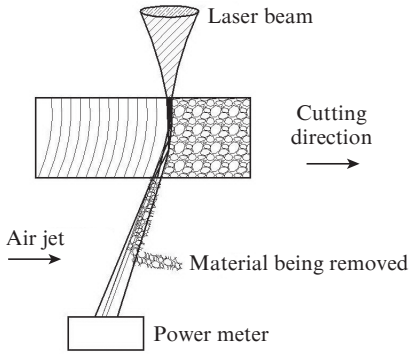

Figure 1. Scheme of measuring the absorption coefficient of the laser beam in the cut channel.

to ensure the highest possible cut quality. The sheets of a thickness of 5 mm were cut using a lens with a focal length of 127 and 190.5 mm in the case of the CO_2 laser, and 150 and 200 mm in the case of the fibre laser. The minimal roughness value obtained in cutting with each pair of lenses was approximately the same (with experimental scatter of data of no more than 10%). Thereafter, all the experiments were performed using a 200 mm lens in the case of the fibre laser and a 190.5 mm lens for the CO_2 laser.

Figure 2 shows the photographs of burning through a vinyl plastic plate by means of the laser beam passed through a focusing lens without cutting and during the cutting after the beam left the cut channel. The prints are made in front of the receiving area of the power meter at a distance of 150 mm from the bottom surface of the cut sheet at a cutting speed of 0.8 m min^{-1}.

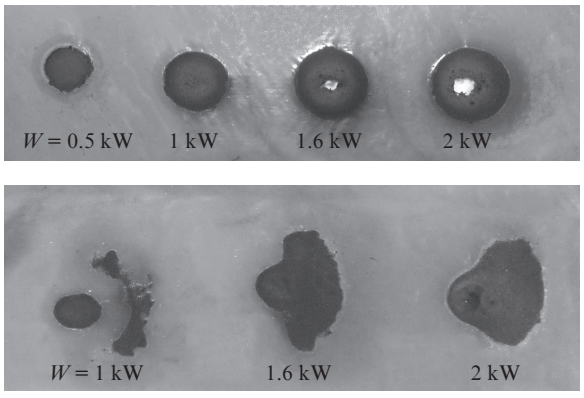

Figure 2. Photographs of burning through a vinyl plastic plate by means of a laser beam: (a) without cutting and (b) during the cutting after exiting from the cut channel.

All the prints are made with the exposure time of 2 s. With 0.5 kW power, the burning-through is not observed. The photographs show that the spatial structures of the beams without cutting and during the cutting process are substantially different. During the cutting process, part of the beam passes through the cut channel without interaction with the material. This part of the beam corresponds to a compact spot, the centre of which coincides with the spot centre in the case of free beam propagation without cutting. Another part of the beam reflects from the cut front; it corresponds to a

spot being offset from the beam axis in the opposite direction to the cutting direction and elongated transversely. The offset magnitude depends on the cutting speed. By means of the heat-sensitive paper, the position of the low-intensity peripheral portion of the beam is accurately defined, and the position of the power meter is corrected to ensure the penetration of the entire spot into the measuring system.

Figure 3 shows the results of measuring the absorption coefficient for the fibre and CO_2 lasers in the form of functions of the cutting speed at different radiation power and the sheet thickness $h = 5$ mm. It is seen that, both for the fibre and CO_2 lasers, the absorption coefficient depends linearly on the cutting speed at a given radiation power, and decreases with increasing power at the same cutting speed for both lasers. Note that, at the same cutting parameters (with radiation power greater than 0.5 kW), the absorption coefficients for the two lasers are close within 10%.

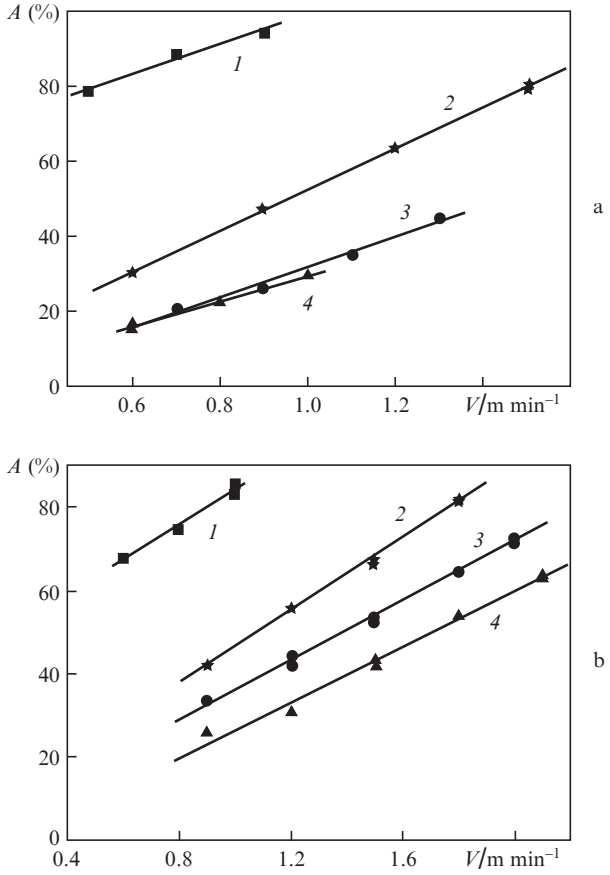

Figure 3. Dependence of the absorption coefficient on the cutting speed and laser power for (a) the fibre laser and (b) CO_2 laser at $W = (1)$ 0.5, (2) 1.0, (3) 1.6 and (4) 2.0 kW; $h = 5$ mm.

However, with account for the cut quality, we arrive at a fundamentally different result. The radiation absorption coefficients for the fibre and CO_2 lasers turn out significantly different when compared not at the same cutting speed but at the optimal cutting speeds that ensure minimality of the cut surface roughness for relevant lasers. As a result of optimisation, the optimal speed V^*, the optimal constriction position and the corresponding cut width b^* at which the surface roughness is minimal are determined. The second condition is the absence of burrs. Figure 4 shows the optimal speed V^* as

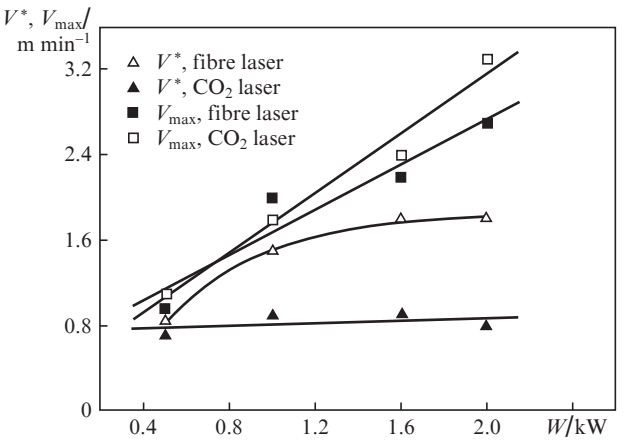

Figure 4. Optimal and maximal speed of cutting by means of radiation from the fibre and CO_2 lasers; $h = 5$ mm.

function of the laser power at $h = 5$ mm. The maximum cutting speed V_{max} is also shown. It is seen that the maximum cutting speeds for the two lasers are approximately equal and depend similarly on the laser power. However, the optimal speeds are significantly different in magnitude and their dependence on the laser power. In the case of the CO_2 laser, the optimal speed increases with increasing power; at a low power this speed is only slightly less than the maximum speed and tends to saturation with increasing power. In the case of the CO_2 laser, the difference between the maximum speed and the speed ensuring a high-quality cut is not too large; this fact has also been reported in [6]. However, in cutting by means of the fibre laser radiation, the optimal speed providing minimal roughness remains constant in the power range of 0.5–2 kW. At a power of 2 kW, the maximal speed is three times greater than the optimal one.

Optimal speeds, cut widths (for a given power) and relevant absorption coefficients have been measured at the thicknesses of 3, 10 and 16 mm. Figure 5 demonstrates the dependence of the laser power being absorbed in the cut channel on the power at the channel entrance under optimal cutting conditions. The power magnitude is normalised here to the sheet thickness h. It can be seen that, if the value W/h is taken as a variable, this dependence is different for the two laser types

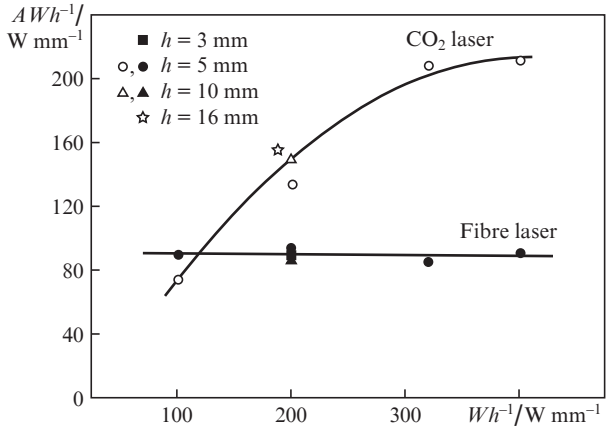

Figure 5. Absorbed laser power at the optimal cutting speed vs. power at the channel entrance; the power is normalised by the cut sheet thickness.

and does not depend on the sheet thickness. In the case of the fibre laser, both the optimal speed and the relevant absorbed power remain constant with increasing input power at the entrance into the cut channel, whereas, in the case of the CO_2 laser, the absorbed power increases with increasing input power, though, at high power densities ($W/h \geqslant 300$ W mm^{-1}), saturation is observed.

Figure 6 shows the results of optimisation in the coordinates AW/h and V^*b^*. It can be seen that the data for the CO_2 laser at different thicknesses can be well approximated by a single linear dependence, whereas the data for the fibre laser occupy a compact region located on this line. The line slope in Fig. 6 gives the absorbed laser energy $E_{abs} = AW/(V^*b^*h)$ per unit volume of the material being removed from the cut channel, in the case that the cut parameters correspond to a minimal roughness. It is seen from Fig. 6 that the values E_{abs} for the fibre and CO_2 lasers are close. The E_{abs} value, averaged over the entire set of data, is equal to 10.9 J mm^{-3} for cutting with the fibre laser and 12.7 J mm^{-3} for cutting with the CO_2 laser. The difference between these values lies within the limits of the experimental error.

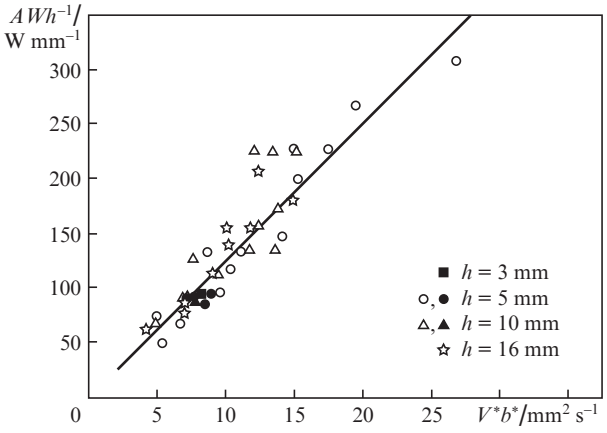

Figure 6. Experimental data corresponding to minimal roughness in the coordinates AW/h and V^*b^*; filled symbols show the data for the fibre laser, and unfilled symbols – data for the CO_2 laser.

4. Discussion of the results

The generalised result of this study can be formulated as follows: minimal roughness of the cut in laser-oxygen cutting of low-carbon steel can be attained at the value of absorbed laser energy $E_{abs} = 11-13$ J mm^{-3} being injected into the unit volume of the material being removed from the cut channel. It is important to emphasise that the E_{abs} value is the same for the fibre and CO_2 lasers. The minimal value of roughness is different for the two lasers – at the sheet thickness of 5 mm, the roughness R_a (arithmetic mean of inhomogeneities) is 2–3 μm in the case of the CO_2 laser and 5–6 μm in the case of the fibre laser. The optimal cutting speed and its dependence on the laser power are also significantly different for the two lasers; nevertheless the E_{abs} value remains constant and does not depend on the laser radiation wavelength and thickness of the cut sheet.

Specific absorbed energy is defined for optimal rather than for maximal cutting speed, and therefore it cannot be regarded as the energy required for material melting. Laser-oxygen cutting of steel represents a forced combustion of iron in oxygen [15]. In the exothermic reaction of iron oxidation, extra energy is allocated and chemical composition of the material in the cutting zone is changed, so that the melt consists predominantly of a mixture of FeO and Fe [15, 16]. It can be assumed that there exists an optimal melt temperature exceeding the melting point of FeO and Fe, at which the surface roughness of the cut is minimal. Various physical processes (their survey is given, for example, in [17]) participate in the formation of the surface of laser cutting, and the dependence of the height of surface ripples on the melt temperature may be different for different processes.

The melt temperature can be estimated from the power balance in the channel of the laser cut, which can be written in the form [18, 19]:

$$AW + W_{ox} = W_{melt} + W_{cond}, \quad (1)$$

where W_{ox} is the power released in exothermic oxidation of iron; W_{melt} is the power consumed for heating and melting of the material being removed; and W_{cond} is the power loss on the sample heating due to the heat relase from the cutting zone due to thermal conduction. The power losses also include the losses due to convective cooling of the sample by an auxiliary gas stream and the power spent on material evaporation. The energy losses on evaporation of the material in laser cutting are small compared to those spent on melting, and they are commonly neglected. The power losses in convective cooling also significantly affect the power balance [19, 20]. Thus, the thermal power losses spent on heating a sample can be treated as the only channel of energy losses not associated with melting and heating of the material that is removed from the channel. Thermal losses during the laser cutting are numerically calculated in [21]. The following approximation is proposed for the Péclet numbers in the range $0.2 \leqslant \mathrm{Pe} \leqslant 10$: $W_{cond} = 3.2k_m h\Delta T \mathrm{Pe}^{0.868}$, where k_m is thermal conductivity and $\Delta T = T - T_m$ is the melt temperature excess above the melting point of the material. Accordingly, equation (1) can be written as:

$$AW + Vhb\rho k_{ox}\Delta H = Vhb\rho(C_{sm}\Delta T_m + C_{lm}\Delta T + L_m) + 3.2k_m h\Delta T_m \mathrm{Pe}^{0.868}. \quad (2)$$

Here, b is the cut width; ρ is the material density; k_{ox} is the mass fraction of iron oxidised in the cutting process; ΔH is the specific thermal capacity of the exothermic oxidation reaction of iron; C_{sm} is the specific thermal capacity; C_{lm} is the specific thermal capacity of the melt substance; $\Delta T_m = T_m - T_0$; T_0 is the environmental temperature; and L_m is the latent heat of fusion.

Relation (2) allows us to determine the excess of the volume-averaged melt temperature over the melting point of the material:

$$\Delta T = \frac{1}{C_{lm}}\left[\frac{E_{abs}}{\rho} + k_{ox}\Delta H - L_m - C_{sm}\Delta T_m(1 + 3.2\mathrm{Pe}^{-0.132})\right]. \quad (3)$$

It is seen that ΔT weakly depends on the Péclet number and is mainly defined by the bulk density of absorbed laser energy and proportion of oxidised iron, whereas other values represent the characteristics of the substance.

The values E_{abs} and k_{ox} are interrelated, and the growth of one of them causes the growth of the other. The values of melt

temperature, oxidation rate, thickness of oxide film on the surface, and proportion of FeO in the melt increase with increasing E_{abs}. The increase in oxide concentration leads to an increase in absorption coefficient, E_{abs} and melt temperature.

The process of iron oxidation in laser-oxygen cutting is cyclical. The cut front propagation occurs in the form of periodically arising and damped combustion waves [13, 15, 16], which propagate both in the direction of cutting and in the lateral direction, creating periodical grooves on the cut's lateral surface. The oxidation reaction rate increases with temperature [22], herewith the linear speed of the cut front and the depth of grooves on the cut's lateral surface also increase. Since, according to (3), the melt temperature is directly related to the magnitude of absorbed laser energy, the depth of grooves increases with increasing E_{abs}.

The impact of the nonstationary nature of the cut front propagation in the form of combustion waves on the surface structure manifests itself to the greatest extent in the upper part of the cut, where the melt film thickness is not large. When the melt flows along the cut front, the film thickness and the melt mass increase, and the hydrodynamic phenomena at the lower part of the cut begin to play a significant role. To ensure a high cut quality, the melt should be effectively removed from the cut channel by means of a gas jet. If the melt viscosity is too high, and the melt possesses high surface tension, the melt accumulates at the cut bottom, thus creating solidified ripples on the cut's lateral surface [17]. Furthermore, if the surface tension of the melt is sufficiently large, a part of the melt is not whirled away from the bottom sheet edge, but remains in the form of solidified droplets and creates a burr. The ratio of capillary and inertial forces in the melt is characterised by the Weber number We, which, for a melt flow in the laser cut channel, can be written in the form [23]:

$$\mathrm{We} = \frac{h_m \rho_m V_m^2}{\sigma}, \tag{4}$$

where σ is the surface tension of the melt material, h_m is the melt film thickness, ρ_m is the melt density, and V_m is the melt flow rate.

The burr arises at too small Weber numbers. To ensure the burr absence, the Weber number of the melt for the lower part of the cut must exceed a certain critical value [23]. Both viscosity and coefficient of surface tension of the melt consisting of a mixture of fluidal FeO and Fe decrease with increasing melt temperature [16]. In this case, the melt is more effectively removed from the cut channel, and the amount of solidified metal and oxides, which is left on the walls and the lower edge of the cut in the form of ripples and burr, turns out less. It is due to the presence of FeO that effective removal of the melt is ensured, since fluidal FeO has a lower viscosity and a significantly lower surface tension compared to Fe at the same temperature [15, 16]. The proportion of FeO in the melt increases with increasing oxidation rate and melt temperature.

Thus, a change in the contribution of the specific laser energy volume causes a change in temperature and chemical composition of the melt in the cut channel. The increase in ripples on the cut surface may be induced by an increase in E_{abs} with a relevant increase in temperature and proportion of FeO, and also by their decrease. The increase in temperature results in the growth of the depth of grooves associated with nonstationary propagation of the cut front in the form of periodically arising waves of burning. With decreasing temperature and proportion of FeO, removing the viscous melt from the cut channel becomes inefficient, thus creating ripples on the lateral wall and lower edge of the cut during the solidification process. Minimal roughness is attained at a certain optimal value of E_{abs}.

5. Conclusions

1. We have measured the absorption coefficient of laser radiation in laser-oxygen cutting of low-carbon steel sheets with a thickness of 3, 5, 10 and 16 mm by means of the fibre and CO_2 lasers. At the sheet thickness of 5 mm, for both lasers the absorption coefficient increases almost linearly with increasing cutting speed and decreases with increasing power at a constant speed.

2. For the fibre and CO_2 lasers, the laser power being absorbed in the regime of optimal cutting, when the surface roughness is minimal, has been determined. In the case of the CO_2 laser, the laser power absorbed in the cut channel, normalised to the plate thickness, increases with increasing power and tends to saturation, while, in the case of the fibre laser, the absorbed power in the optimal regime remains invariable with increasing input power at the channel entrance.

3. In laser-oxygen cutting of low-carbon steel, the surface roughness of the cut attains its minimum provided that the absorbed laser energy per unit volume of the material being removed from the cut channel is constant. This energy has the same value (11–13 J mm^{-3}) in cutting by means of radiation from the fibre and CO_2 lasers in the thickness range of 3–16 mm.

4. A qualitative explanation of the existence of an optimal value of the absorbed laser energy is proposed. With increasing absorbed energy and melt temperature, the surface roughness increases due to an increase in the amplitude of periodically arising combustion waves and decreases due to a decrease in viscous and capillary forces and more efficient removal of the melt from the cut channel.

References

1. Powell J., Kaplan A.F.H. *Proc. 31st International Congress on Applications of Lasers & Electro-Optics* (Anaheim, CA, USA, 2012) p. 277.
2. Stelzer S., Mahrle A., Wetzig A., Beyer E. *Physics Procedia*, **41**, 399 (2013).
3. Scintilla L.D., Tricarico L., Wetzig A., Beyer E. *Int. J. Mach. Tools Manuf.*, **69**, 30 (2013).
4. Petring D., Shneider F., Wolf N. *Proc. 31st International Congress on Applications of Lasers & Electro-Optics* (Anaheim, CA, USA, 2012) p. 43.
5. Mahrle A., Beyer E. *J. Phys. D: Appl. Phys.*, **42**, 175507 (2009).
6. Petring D., Shneider F., Wolf N., Nazery V. *Proc. 27th International Congress on Applications of Lasers & Electro-Optics* (Temecula, CA, USA, 2008) p. 95.
7. Hirano K., Fabbro R. *J. Laser Appl.*, **24**, 012006 (2012).
8. Scintilla L.D., Tricarico L., Mahrle A., Wetzig A., Himmer T., Beyer E. *Proc. 29th International Congress on Applications of Lasers & Electro-Optics* (Anaheim, CA, USA, 2010) p. 249.
9. Pocorni J.K., Petring D., Powell J., Deichsel E., Kaplan A.F.H. *Proc. 33rd International Congress on Applications of Lasers & Electro-Optics* (San Diego, CA, USA, 2014) p. 905.
10. Afonin Yu.V., Golyshev A.P., Ivanchenko A.I., Malov A.N., Orishich A.M., Pechurin V.A., Filev V.F., Shulyat'ev V.B. *Kvantovaya Elektron.*, **34**, 307 (2004) [*Quantum Electron.*, **34**, 307 (2004)].
11. Malikov A.G., Orishich A.M., Shulyatyev V.B. *Int. J. Mach. Tools Manuf.*, **49**, 1152 (2009).
12. Malikov A.G., Orishich A.M., Shulyat'ev V.B. *Kvantovaya Elektron.*, **39**, 547 (2009) [*Quantum Electron.*, **39**, 547 (2009)].

13. Miyamoto I., Maruo H. *Weld. World*, **29**, 283 (1991).
14. Malikov A.G., Orishich A.M., Shulyat'ev V.B. *Kvantovaya Elektron*., **42**, 640 (2012) [*Quantum Electron*., **42**, 640 (2012)].
15. Powell J., Petring D., Kumar R.V., Al-Mashikhi S.O., Kaplan A.F.H., Voisey K.T. *J. Phys. D: Appl. Phys.*, **42**, 015504 (2009).
16. Ivarson A., Powell J., Kamalu J., Magnusson C. *J. Mater. Process. Tech.*, **49**, 359 (1994).
17. Dahotre N.B., Harimkar S.P. *Laser Fabrication and Machining of Materials* (New York: Springer, 2008) p. 171.
18. Ready J.F. (Ed.) *LIA Handbook of Laser Materials Processing* (Orlando: Magnolia Publishing Inc., 2001) p. 428.
19. Steen W. *Laser Material Processing* (London: Springer-Verlag, 2003).
20. Bazyleva I.O., Galushkin M.G., Golubev V.S., Dubrovin E.A., Karasev V.A. *Sbornik trudov IPLIT 'Sovremennye laserno-informatsionnye tekhnologii'* (Proc. Institute on Laser and Information Technologies, RAS 'Modern Laser-Information and Laser Technologies') (Moscow: Interkontakt Nauka, 2005) p. 221.
21. Prusa J.M., Venkitachalam G., Molian P.A. *Int. J. Mach. Tools Manuf.*, **39**, 431 (1999).
22. Bunkin F.V., Kirichenko S.A., Luk'yanchuk B.S. *Kvantovaya Elektron*., **9**, 1959 (1982) [*Sov. J. Quantum Electron*., **12**, 1276 (1982)].
23. Riveiro A., Quintero F., Lusquinos F., Comesana R., Pou J. *J. Phys. D: Appl. Phys*., **44**, 135501 (2011).